Research Article

Journal of PeptideScience

Received: 20 October 2009 Accepted: 30 November 2009 Published online in Wiley Interscience: 28 January 2010

(www.interscience.com) DOI 10.1002/psc.1208

Conformational properties of the residues connected by ester and methylated amide bonds: theoretical and solid state conformational studies

Dawid Siodłak* and Anna Janicki

Peptides produced by bacteria and fungi often contain an ester bond in the main chain. Some of them have both an ester and methylated amide bond at the same residue. A broad spectrum of biological activities makes these depsipeptides potential drug precursors. To investigate the conformational properties of such modified residues, a systematic theoretical analysis was performed on *N*-acetyl-L-alanine *N*′-methylamide (Ac-Ala-NHMe) and the analogues with the ester bond on the *C*-terminus (Ac-Ala-OMe), *N*-terminus (Ac-[psi](COO)-Ala-NHMe) as well as the analogues methylated on the *N*-terminus (Ac-(Me)Ala-OMe) and *C*-terminus (Ac-[psi](COO)-Ala-NMe_2). The ϕ, ψ potential energy surfaces and the conformers localised were calculated at the B3LYP/6-311++G(d,p) level of theory both *in vacuo* and with inclusion of the solvent (chloroform, water) effect (SCRF method). The solid state conformations of the studied residues drawn from The Cambridge Structural Database have been also analysed. The residues with a *C*-terminal ester bond prefer the conformations β, C5, and α_R, whereas those with *N*-terminal ester bond prefer the conformations β, α_R, and the unique conformation α' ($\phi, \psi = -146^\circ, -12^\circ$). The residues with *N*-terminal methylated amide and a *C*-terminal ester bond prefer the conformations β, $\beta 2$, and interestingly, the conformation α_L. The residues with a *C*-terminal methylated amide and an *N*-terminal ester bond adopt primarily the conformation β. The description of the selective structural modifications, such as those above, is a step towards understanding the structure-activity relationship of the depsipeptides, limited by the structural complexity of these compounds. Copyright © 2010 European Peptide Society and John Wiley & Sons, Ltd.

Keywords: depsipeptide; methylation; conformational analysis; X-ray structure; DFT calculations

Introduction

Depsipeptides can be defined as compounds containing amino acid and hydroxy acid residues connected by amide and ester bonds [1,2]. This structural modification is often found in small, cyclic peptides produced primarily by bacteria and fungi or isolated from marine invertebrates, such as molluscs, sponges, ascidians and jellyfishes. Depsipeptides reveal very a broad spectrum of biological activities: antibiotic, antifungal, anti-inflammatory, anti-tumour, immunosuppressive and combating HIV. Thus, many of them are perceived as potential drug precursors [3,4].

The majority of depsipeptides contain only one ester bond, for example, FR901228 [5], azinothricins [6], taumycins [7], myxochromide [8], zygosporamide [9] and sansalvamide [10]. However, there are compounds that contain an equal or even greater number of ester bonds as compared to peptide bonds, like valinomycin [11], cereulide [12] and montanastatin [13].

Apart from the ester bond in the main chain, the depsipeptides contain many other structural modifications. Methylation of amide is the one that occurs most commonly. The ester and methylated amide bonds can be separated by more than one residue, as in the case of destruxins [14], polydiscamides [15], somamides [16], micropeptins [17], oscillapeptin [18], geodiamolides [19] and eujavanicin A [20]. Very often, these modifications are present at the same residue. The methylathed amide can occur at the *N*-terminus of the given residue, while the ester bond is present at the *C*-terminus. This is the case for theonellapeptolides [21], callipeltins [22], stereocalpin A [23], celebesides [24], yanucamides [25], luzopeptins [26], hantupeptin A [27] and tamandarins A and B [28]. The reversed order of the neighbouring ester and methylated amide bonds can be found in spongidepsin [29], petriellin A [30], malevamides [31] and carriebowmide [32]. There are also compounds, like enniatins [33], beauvericin, bassianolide, PF1022A [34,35] and verticilide [36], where the residues are connected alternately by the ester and methylathed amide, and the typical peptide bond is not present. Finally, almost all combinations of the ester, amide or methylated amide bonds are present in compounds such as aureobasidins [37], dolastatin D [38], dolastatin 17 [39] and wewakpeptins [40].

Therefore, it is worth investigating how the ester bond that joins the residues in the main chain influences their conformational properties. It can also be assumed that the residues connected by both ester and methylated amide will have their own conformational preferences, which depend on the mutual position of these neighbouring groups.

Despite the natural occurrence of the depsipeptides and their usefulness as potential drugs, there is limited literature on the systematic analysis of the conformational properties of the residues

* *Correspondence to: Dawid Siodłak, Faculty of Chemistry, University of Opole, Opole, Poland. E-mail: dsiodlak@uni.opole.pl*

Faculty of Chemistry, University of Opole, Opole, Poland

Journal of PeptideScience

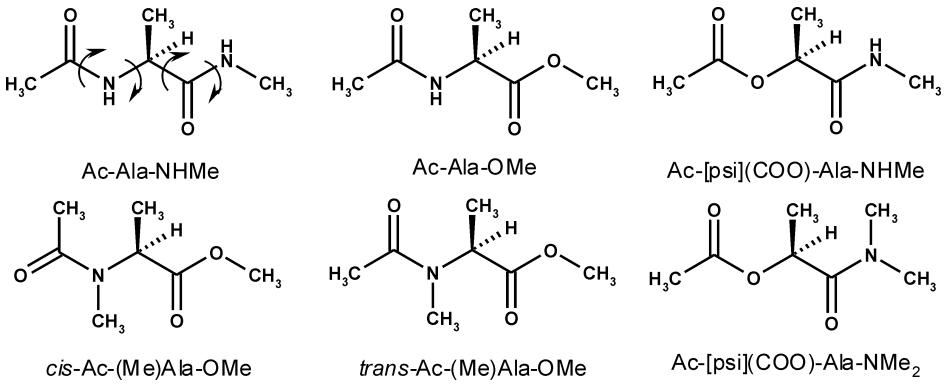

Figure 1. General formula of the model compounds containing the residues studied in this work.

connected by the ester group [41–44]. The latest theoretical conformational study focuses on *N*-acetyl-*N*′-methylamide of L-lactic acid (Ac-Lac-NHMe), with the depsidipeptide having the ester bond at the *N*-terminus of the affected residue. It was found that the most preferred conformations are the polyproline II helical conformation ($\phi \sim -70^{\circ}$, $\psi \sim 150^{\circ}$) and the conformation of the torsion angles about $\phi \sim -150^{\circ}$, $\psi = \sim 0^{\circ}$ [43,44]. The ester bonds reveal a negligible tendency to adopt the configuration *cis* [44]. The residues having both ester and methylated amide linkages were not investigated.

In order to obtain a more comprehensive view on the influence of the ester group as well as ester, and the neighbouring methylated amide on the conformational preferences of the modified residues, two methods were used in this study: a theoretical analysis of the depsidipeptide molecules and a search of solid state conformations of the structurally analogous residues of depsipeptides gathered in The Cambridge Structural Database [45].

Depsipeptides are peptide analogues, where the CONH group that joins residues is replaced by the ester group. To study the influence of the ester group on the conformational properties of the given residue in the main chain, it is preferable not to differentiate between the amino acid residues and hydroxy acid residues, but the latter perceive as the amino acid residues modified at the *N*-terminus, particularly since most of them have a side chain of standard amino acids. They can be indicated by placing a Greek psi, followed by the replacing ester group in parenthesis, between the residue symbols where the change occurs (-[psi](COO)Xaa-) [46].

Table 1. The standard and modified amino acids residues with ester and methylated amide linkages drawn from The Cambridge Structural Database

Residue	L-form	D-form	Total
-CO-Ala-NH-	667 (85%)	122 (15%)	789
-CO-Xaa-NH-	2262 (85%)	386 (15%)	2648
-CO-Xaa-O-(C)	863 (81%)	195 (19%)	1048
-[psi](COO)Xaa-NH-	68 (50%)	69 (50%)	137
trans-CO-(Me)Xaa-O-(C)	49 (86%)	8 (14%)	57
trans-CO-(R)Xaa-O-(C)	105 (83%)	22 (17%)	127
cis-CO-(Me)Xaa-O-(C)	9 (64%)	5 (36%)	14
cis-CO-(R)Xaa-O-(C)	23 (72%)	9 (28%)	32
-[psi](COO)Xaa-NMe-	11 (18%)	49 (82%)	60
-[psi](COO)Xaa-NR-	28 (36%)	49 (64%)	77

Experimental Methods

Theoretical Calculation

The conformational properties of depsipeptides were studied on the basis of the following molecules: Ac-Ala-NHMe, Ac-Ala-OMe, Ac-[psi](COO)-Ala-NHMe, Ac-(Me)Ala-OMe and Ac-[psi](COO)-Ala-NMe$_2$ (Figure 1). The Gaussian 03 program was used [47]. Calculations were performed on the *trans*-amide and *trans*-ester bonds ($\omega_0, \omega_1 \sim 180^{\circ}$), except for the Ac-(Me)Ala-OMe molecules where both configurations, *trans* and *cis*, of the methylated *N*-terminal amide bond were considered. The ϕ, ψ potential energy surfaces of the studied molecules were created on the basis of 144 points calculated at the B3LYP/6-311++G** level of theory with a 30° increment for the ϕ, ψ main-chain dihedral angles. The energy surfaces were obtained using the Surfer 8 program with the radial basis function as a gridding method (Golden Software, Inc., 2002). To estimate the effects of environment on the shapes of the energy surfaces, single-point calculations were conducted in each grid point using a self-consistent reaction field (SCRF) model. The polarisable continuum model (PCM) was chosen [48,49]. The possible energy minima of every low-energy region of the potential energy surfaces were checked by full geometry optimisation of the selected structure at the B3LYP/6-311++G** level *in vacuo* as well as in the chloroform and water mimicking environment using the PCM. Frequency analyses were carried out to verify the nature of the minimum state of all the stationary points obtained and to calculate the zero-point vibrational energies (ZPVEs) and both thermal and entropic corrections.

Crystal Structure Database

On the basis of the data gathered in The Cambridge Structural Database (CSD) of The Cambridge Crystallographic Data Centre [45], the conformational properties of the amino acid residues with the *C*-terminal or *N*-terminal ester bond, and again, with the ester bond and methylated amide bond were studied. The following structures were analysed: -CO-Ala-NH-, -CO-Xaa-NH-, -CO-Xaa-O-(C), -[psi](COO)-Xaa-NH-, -CO-(Me)Xaa-O-(C), -CO-(R)Xaa-O-(C), -[psi](COO)-Xaa-NMe- and -[psi](COO)-Xaa-NR-, where Xaa describes standard amino acid residue, except glycine and proline (Table 1). To increase the amount of data, not only the configuration L of the C^{α} carbon atom but also the configuration D was considered. In the latter case, the signs of the ϕ, ψ torsion angles were inverted.

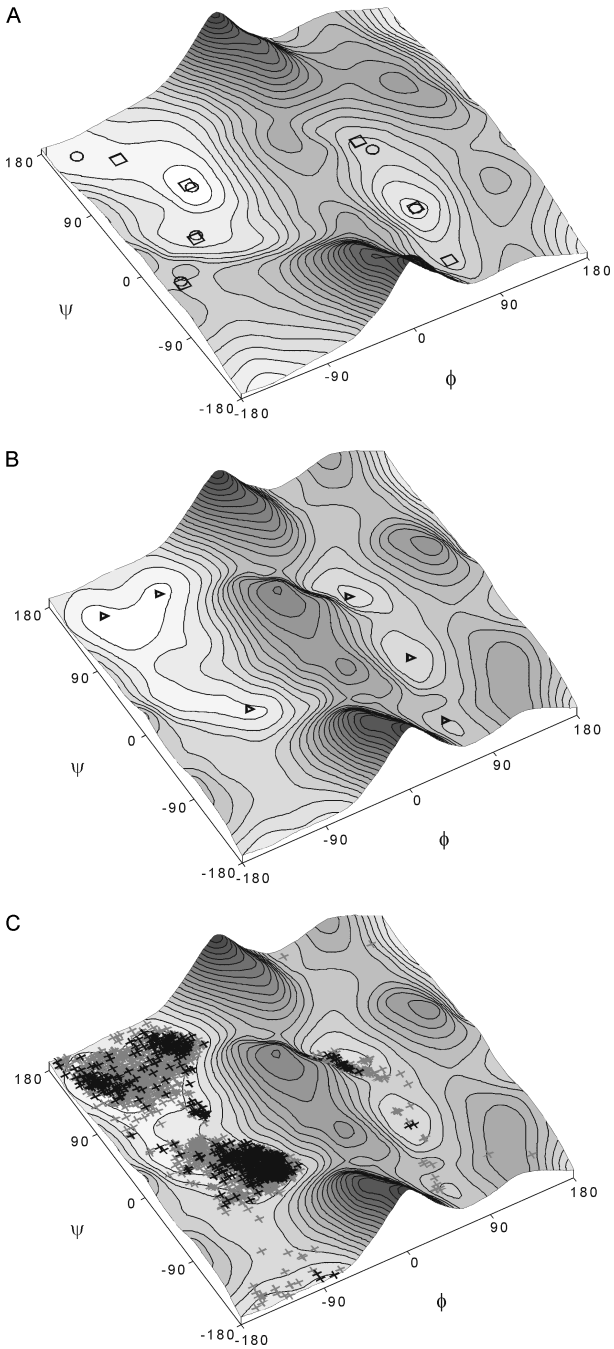

Figure 2. The ϕ, ψ potential energy surfaces of the Ac-Ala-NHMe molecule: (a) plot calculated *in vacuo*, conformers calculated both *in vacuo* (○) and in a chloroform mimicking environment (□), (b) plot and conformers in a water mimicking environment and (c) distribution of the solid state conformations of the alanine (-CO-Ala-NH-) residue (**+**) and standard (-CO-Xaa-NH-) non-Gly, non-Pro residues (+) depicted on the plot calculated in a water mimicking environment.

Table 2. Conformers of the Ac-Ala-NHMe molecule

Conformer	ϕ (°)	ψ (°)	Energy (Hartrees)	ΔE (kcal/mol)
in vacuo				
C7eq	−83.5	76.0	−495.826207	0.00
C5	−155.0	159.2	−495.825134	0.68
$\beta 2$	−115.1	13.6	−495.822498	2.33
C7ax	73.1	−56.1	−495.822136	2.56
α_L	72.0	19.7	−495.818051	5.12
α'	−164.6	−44.7	−495.816409	6.15
Chloroform mimicking environment				
C5	−125.7	135.5	−495.841311	0.00
C7eq	−85.6	80.7	−495.840141	0.73
$\beta 2$	−117.5	9.7	−495.837877	2.15
C7ax	73.5	−55.1	−495.836783	2.84
α_L	65.1	34.4	−495.835102	3.89
α_D	61.1	−137.7	−495.833473	4.92
α'	−164.7	−48.2	−495.832289	5.66
Water mimicking environment				
C5	−142.1	144.5	−495.851145	0.00
β	−84.6	141.3	−495.851122	0.01
α_R	−83.8	−25.5	−495.849838	0.82
α_L	61.5	41.0	−495.847409	2.34
C7ax	73.1	−53.3	−495.844384	4.24
α_D	59.3	−142.0	−495.843768	4.63

Results and Discussion

Ac-Ala-NHMe

Figure 2 presents the conformational maps for the Ac-Ala-NHMe molecule, the standard alanine model, together with its conformers. For the calculation performed *in vacuo* six conformers can be found in the following order of stability: C7eq, C5, $\beta 2$, C7ax, α_L, and α' (Table 2, Figure 2(a)). The number of the conformers, the values of their torsion angles ϕ, ψ, and their relative stabilities correspond to those found earlier by using various computational methods [[50] and ref. into]. When the effect of a weakly polar chloroform environment is considered, the additional conformer α_D can be seen. The relative energy order and the value of the torsion angles do not result in considerable changes, except for the conformer C5, which shifts deeper inside the map and becomes the conformer lowest in energy. The calculations using a water mimicking environment results in greater changes (Figure 2(b)). The conformers C7eq, $\beta 2$ and α' disappear. Instead, the conformer β and α_R can be seen. The six conformers are present in the following order of stability: C5, β, α_R, α_L, C7ax and α_D. The difference in energy between three lowest conformers, C5, β, α_R, does not exceed 1 kcal/mol.

Figure 2(c) presents distribution of the ϕ, ψ angles of 789 alanine residues, -CO-Ala-NH-, (marked black crosses) and 2648 remaining standard, non-Gly, non-Pro amino acids residues (marked grey crosses), -CO-Xaa-NH-, found in The Cambridge Structural Database. As can be seen, the distribution of the solid state conformations fits to the calculations preformed in the water mimicking environment. They are placed in the regions of the calculated conformers. The largest number of solid state conformations was found for the conformers of the lowest energy, C5, β and α_R. The distribution of the alanine residues fits more closely to the position of the calculated conformers, whereas the distribution of the remaining standard residues is broader. The overall shape of the distribution of the solid state conformers corresponds to the shape of the calculated map. It is also in agreement with the distribution of 81 234 non-Gly, non-Pro and non-prePro residues from 500 high-resolution proteins and the shape of the ϕ, ψ plot created using density-dependent smoothing [51].

The comparison between the distribution of the conformations found in the solid state and the results of the theoretical

Journal of PeptideScience

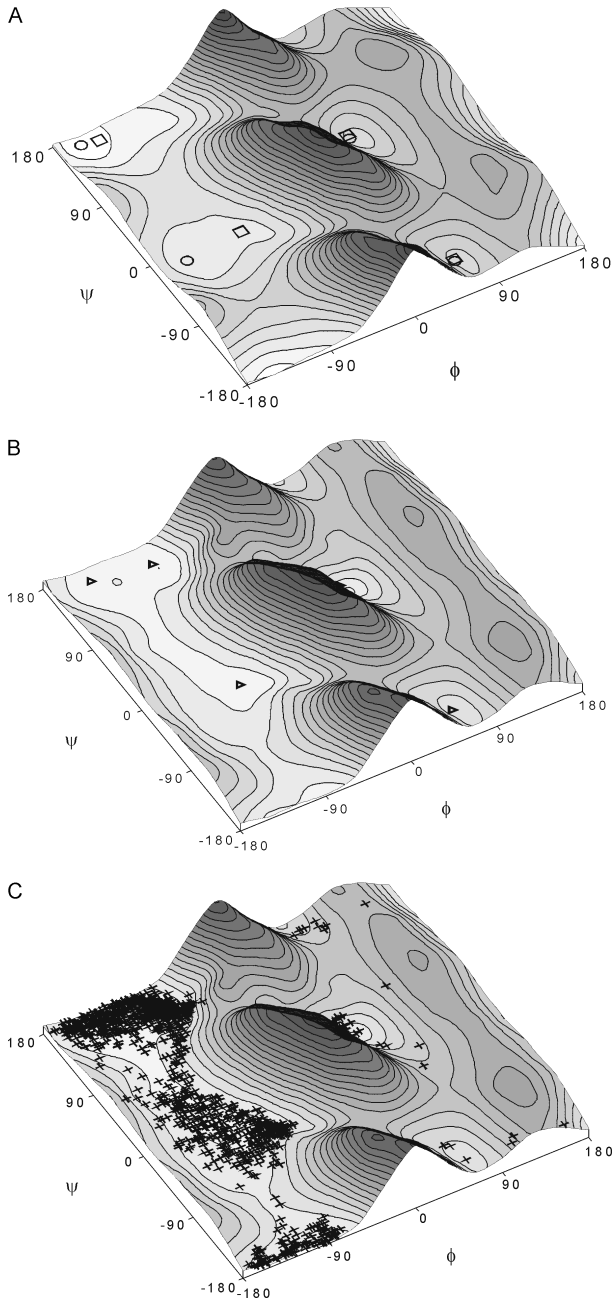

Figure 3. The ϕ, ψ potential energy surfaces of the Ac-Ala-OMe molecule: (a) plot calculated *in vacuo*, conformers calculated *in vacuo* (○) and in a chloroform mimicking environment (□), (b) plot and conformers in a water mimicking environment and (c) distribution of the solid state conformation of the -CO-Xaa-O-(C) residue (non-Gly, non-Pro) presented on the plot calculated in a water mimicking environment.

calculations enable the assumption that the theoretical method applied should correctly predict the conformational preferences of the depsiptide models, for which a much smaller amount of conformational data is accessible.

Ac-Ala-OMe

Figure 3 presents the conformational maps for Ac-Ala-OMe, the model amino acid residue with a *C*-terminal ester bond. The calculation performed *in vacuo* shows four conformers:

Table 3. Conformers of the Ac-Ala-OMe molecule

Conformer	ϕ (°)	ψ (°)	Energy (Hartrees)	ΔE (kcal/mol)
in vacuo				
C5	−155.8	169.3	−515.704382	0.00
α'	−151.0	−18.4	−515.701179	2.01
α_L	54.1	36.0	−515.697860	4.09
α_D	58.4	−151.4	−515.697354	4.41
Chloroform mimicking environment				
C5	−138.5	165.9	−515.715469	0.00
α_R	−89.5	−11.8	−515.713878	1.00
α_L	54.1	40.4	−515.712044	2.15
α_D	58.9	−149.1	−515.711258	2.65
Water mimicking environment				
β	−77.7	158.3	−515.722774	0.00
C5	−138.5	165.4	−515.722226	0.34
α_R	−87.7	−18.4	−515.721514	0.79
α_L	52.9	43.25	−515.720456	1.45
α_D	59.2	−150.4	−515.719429	2.10

C5, α', α_L and α_D, with the most stable conformer being C5 (Table 3, Figure 3(a)). In the chloroform mimicking environment, the conformer α' shifts into the region of the conformer α_R, which becomes second in the energy order. The gap in energy between the conformer lowest in energy, C5, and the conformer α_R, does not exceed 1 kcal/mol. In the water mimicking environment (Figure 3(b)) the conformer β appears and becomes the most stable conformer. The order of the remaining conformers, C5,α_R, α_L and α_D, does not change. It should be noted that there are three low-energy conformers, β, C5 and α_R, and the difference in energy between them is below 1 kcal/mol.

The distribution of the 1048 solid state conformations, -CO-Xaa-O-, fits the shape of the map calculated in the water mimicking environment (Figure 3(c)). It also corresponds both to the position and stability of the calculated conformers. The most occupied areas are those around the lowest conformers β, C5 and α_R. The conformers α_L and α_D have higher energy and only a few solid state conformations correspond to them.

Comparison of the conformational properties of the Ac-Ala-OMe molecule to the standard alanine model indicates that introduction of the ester bond instead of the *C*-terminal amide bond results primarily in the absence of the conformers C7ax and C7eq. For Ac-Ala-NHMe, they were stabilised by the internal, seven-membered N–H···O hydrogen bond, where the *C*-terminal N–H group was donor. For the Ac-Ala-OMe molecule, this stabilising force is not present. The calculation performed *in vacuo* and in the chloroform mimicking environment also revealed the absence of the conformer β2. Nevertheless, in the water mimicking environment the conformers of the Ac-Ala-OMe molecule are similar to those of the standard alanine model, except for the lack of the conformer C7ax. As in the case of Ac-Ala-NHMe, the areas most occupied by the solid state conformations are those of the lowest conformers β, C5 and α_R. Similarly, the conformers highest in energy are α_L and α_D. In the results, the shape of the maps of both the Ac-Ala-NHMe and Ac-Ala-OMe molecules do not differ much, apart from the conformer C7ax. The distribution of the solid state conformation of the -CO-Xaa-NH- and -CO-Xaa-O- residues is also similar. Thus, it can be concluded that the introduction of the

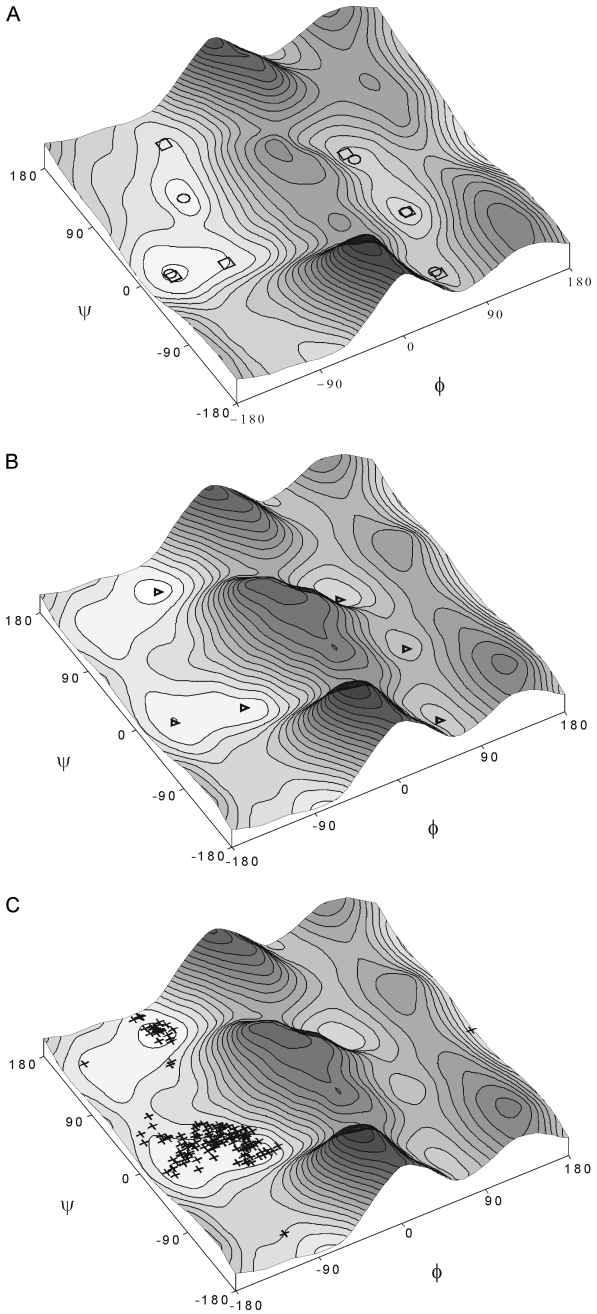

Figure 4. The ϕ, ψ potential energy surfaces of the Ac-[psi](COO)Ala-NHMe molecule: (a) plot calculated *in vacuo*, conformers calculated *in vacuo* (○) and in a chloroform mimicking environment (□), (b) plot and conformers in a water mimicking environment and (c) distribution of the solid state conformation of the -[psi](COO)Xaa-NH- residue (non-Gly, non-Pro) presented on the plot calculated in a water mimicking environment.

ester bond at the *C*-terminus of the affected residues should not have a considerable influence on its conformational properties.

Ac-[psi](COO)-Ala-NHMe

Figure 4 presents the conformational maps for Ac-[psi](COO)-Ala-NHMe, the model of the amino acid residue with an *N*-terminal ester bond. The calculation performed *in vacuo* shows five conformers: α', C7eq, C7ax, α_L and α_D (Table 4, Figure 4(a)). The conformer α' is the lowest in energy. The second in the

Table 4. Conformers of the Ac-[psi](COO)-Ala-NHMe molecule

Conformer	ϕ (°)	ψ (°)	Energy (Hartrees)	ΔE (kcal/mol)
in vacuo				
α'	−147.9	0.3	−515.706915	0.00
C7eq	−88.3	78.1	−515.706053	0.54
C7ax	76.2	−52.9	−515.701117	3.64
α_L	67.9	28.6	−515.700095	4.28
α_D	57.0	−141.0	−515.698254	5.44
Chloroform mimicking environment				
α'	−146.7	−4.4	−515.717948	0.00
β	−71.6	143.7	−515.717809	0.09
α_R	−97.7	−18.3	−515.717303	0.40
α_L	63.7	38.0	−515.712508	3.41
C7ax	77.3	−53.7	−515.710546	4.64
α_D	58.8	−145.5	−515.710148	4.89
Water mimicking environment				
β	−70.8	148.9	−515.726078	0.00
α_R	−80.2	−28.6	−515.725101	0.61
α'	−145.7	−11.6	−515.724882	0.75
α_L	62.7	39.3	−515.720722	3.36
α_D	60.5	−152.0	−515.717751	5.22
C7ax	78.201	−58.8	−515.715006	6.94

energy order is the conformer C7eq. It disappears, however, in the chloroform mimicking environment. Instead, the calculations reveal the conformers β and α_R. The conformer α' is still the most stable, but the gap in energy between the conformers α', β and α_R is very small and does not exceed 0.4 kcal/mol. The water environment does not change the number and the position of the conformers (Figure 4(b)). It changes the energy order, which is as follows: β, α_R, α', α_L, α_D and C7ax. The difference in energy between the three lowest energy conformers, β, α_R and α', does not exceed 0.8 kcal/mol. The conformers α_L, α_D and C7ax are much higher in energy, regardless of the environment.

The search of the CSD database results in 137 solid state conformers of the -[psi](COO)-Xaa-NH- residues (Figure 4(c)). It is a much smaller number than in the case of the standard amino acid residues as well as the residues having *C*-terminal ester bonds. Nevertheless, their distributions correspond to the positions of the three lowest conformers calculated for the polar environment. They occupy the area of the conformers β, α_R and α'. There is no solid state conformation that corresponds to the higher energy conformers α_L, α_D and C7ax.

The absence of the conformer C5, and simultaneously, the appearance of the conformer α' of an unusual stability should be noticed. The conformer α' can be detected for the standard alanine model using calculations performed *in vacuo* and a weakly polar environment. However, for the Ac-Ala-NHMe molecule, it is the conformer of the highest energy. The absence of the conformer C5 results from the lack of the *N*-terminal N–H group, which was the donor of the five-membered N–H···O hydrogen bond. In contrast, similar five-membered N–H···O interaction between the oxygen atom of the *N*-terminal ester bond and the N–H group of the *C*-terminal amide, explains the low energy of the conformer α', which was described earlier (Zhang, Kang). It should be added that such five-membered N–H···O interaction also stabilises the conformer α_R. The change of the torsion angle ϕ, when going from the

Journal of PeptideScience

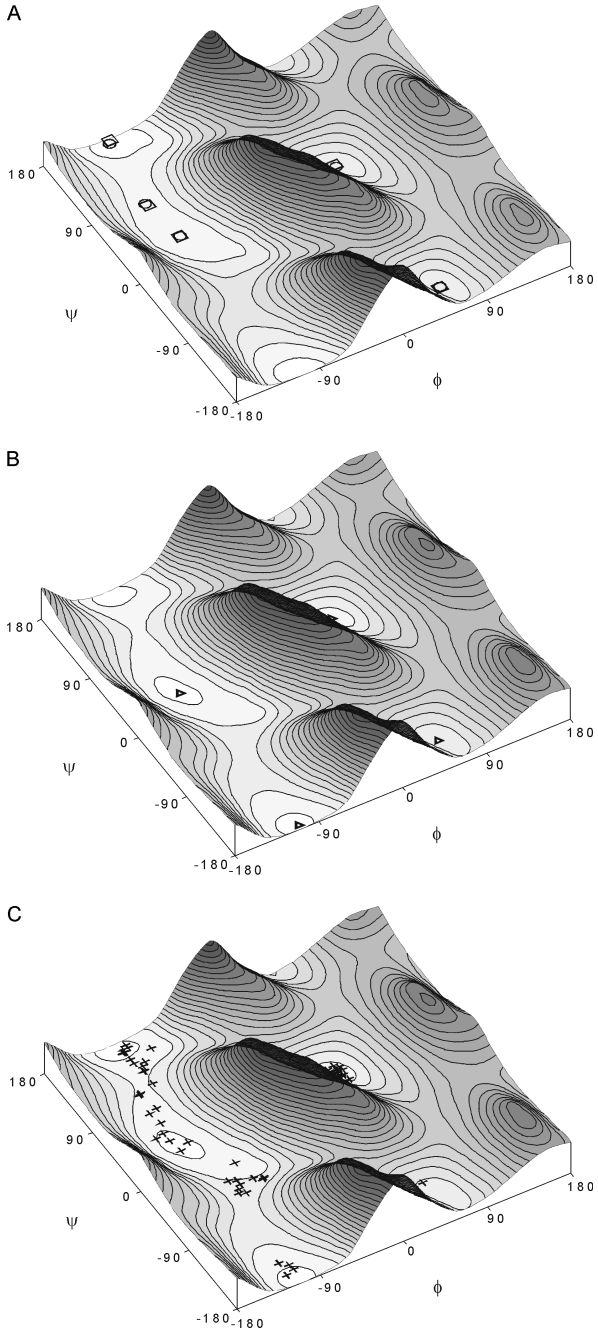

Figure 5. The ϕ, ψ potential energy surfaces of the *trans*-Ac-(Me)Ala-OMe molecule: (a) plot calculated *in vacuo*, conformers calculated *in vacuo* (○) and in a chloroform mimicking environment (□), (b) plot and conformers in a water mimicking environment and (c) distribution of the solid state conformation of the *trans*-CO-(R)Xaa-O-(C) residue (non-Gly, non-Pro) presented on the plot calculated in a water mimicking environment.

conformer α' towards the conformer α_R does not influence the parameter of these stabilising forces. Thus, the flat region enveloped by these two conformers can be seen on the potential surface map.

Trans-Ac-(Me)Ala-OMe

Figure 5 presents the conformational maps for the *trans*-Ac-(Me)Ala-OMe molecule, the model of the residue with a *C*-terminal ester bond, and simultaneously, methylated on the *N*-terminal amide bond having the configuration *trans*. The calculations *in vacuo* and in a chloroform mimicking environment reveal the presence of the five conformers: β, $\beta2$, C7eq, α_L and α_D (Table 5, Figure 5(a) and 5(b)). The conformer C7eq disappears in the water mimicking environment (Figure 5(c)), but the remaining conformers β, $\beta2$, α_L and α_D are constantly present. The environment seems to not influence the order of their stability, and insignificantly, the value of their torsion angles. The gap in energy between the conformers does not exceed 1.5 kcal/mol. The low energy of the conformer α_L should be noted. In the water mimicking environment, the gap in energy between the most stable conformer β and the conformer α_L does not exceed 0.5 kcal/mol. The conformations found in the solid state correspond to all the conformers calculated. The majority of them are placed in a flat valley created by the connected areas of the conformers β and $\beta2$. Again, the conformer α_L should be noted, because 46 of 127 solid state conformations are placed in its region.

Table 5. Conformers of the *trans* Ac-(Me)Ala-OMe molecule

Conformer	ϕ (°)	ψ (°)	Energy (Hartrees)	ΔE (kcal/mol)
in vacuo				
β	−111.7	174.8	−554.983505	0.00
$\beta2$	−116.5	34.8	−554.983152	0.22
C7eq	−124.6	86.2	−554.982029	0.92
α_L	52.9	37.5	−554.981702	1.13
α_D	57.5	−148.2	−554.981271	1.40
Chloroform mimicking environment				
β	−109.4	178.3	−554.993694	0.00
$\beta2$	−117.4	34.4	−554.993579	0.08
α_L	52.6	40.1	−554.992225	0.93
C7eq	−123.5	83.3	−554.992158	0.97
α_D	56.9	−148.7	−554.991282	1.52
Water mimicking environment				
β	−109.0	−174.8	−554.998930	0.00
$\beta2$	−117.7	30.9	−554.998918	0.01
α_L	51.7	42.4	−554.998147	0.49
α_D	56.0	−148.2	−554.997157	1.11

In comparison to Ac-Ala-OMe and Ac-Ala-NHMe, the *trans*-Ac-(Me)Ala-OMe molecule reveals the absence of the conformer α_R, one of the most important and lowest in energy conformers. Furthermore, the conformer C5 is also absent and its region as well as the region of the conformer β are considerably diminished. The conformer β (ϕ, $\psi \sim -110°$, 176°) is present but the values of its torsion angles are deviated from those adopted by the analogous conformers of Ac-Ala-OMe and Ac-Ala-NHMe. The second in the energy order is the conformer $\beta2$ (ϕ, $\psi \sim -117°$, 33°), which is present for the standard alanine residue only *in vacuo* or in the chloroform mimicking environment. This conformer, with its geometry almost unchanged regardless of environment, seems to be an important feature of the residue with a *C*-terminal ester bond and methylated on the *trans* *N*-terminal amide. Another distinguishing feature is the conformer α_L. Its position does not change much in comparison to those for Ac-Ala-OMe and Ac-Ala-NHMe. However, its relative energy is much smaller, and thus, as can be seen by the distribution of the solid state conformation, it becomes one of the most adopted.

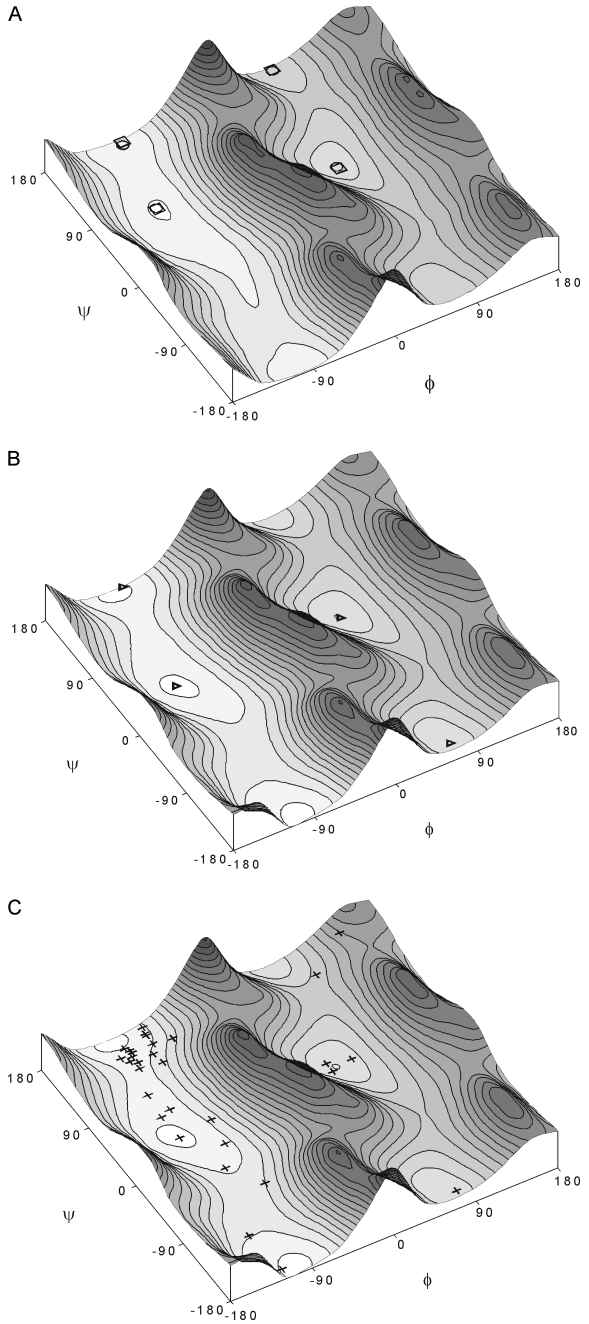

Figure 6. The ϕ, ψ potential energy surfaces of the *cis*-Ac-(Me)Ala-OMe molecule: (a) plot calculated *in vacuo*, conformers calculated *in vacuo* (○) and in a chloroform mimicking environment (□), (b) plot and conformers in a water mimicking environment and (c) distribution of the solid state conformation of the *cis*-CO-(R)Xaa-O-(C) residue (non-Gly, non-Pro) presented on the plot calculated in a water mimicking environment.

The presence of the *C*-terminal ester and methylated *trans* *N*-terminal amide results in the absence of the N–H···O hydrogen bonds, which stabilises the conformer C5 as well as C7. Furthermore, the bulky *N*-methyl group imposes steric hindrance at the higher values of the torsion angle ϕ, which disfavours the extended conformer C5. Similarly, because of the steric hindrance between the bulky *N*-methyl group and the side chain of amino acid residue, it is difficult to adopt the torsion angle ϕ close to the value -80°. As a consequence, the conformer α_R is absent

Table 6. Conformers of the *cis* Ac-(Me)Ala-OMe molecule

Conformer	ϕ (°)	ψ (°)	Energy (Hartrees)	ΔE (kcal/mol)
in vacuo				
C7eq	−111.9	84.4	−554.981238	0.00 (1.42)
β	−97.4	173.4	−554.980747	0.31 (1.73)
α_L	59.5	35.6	−554.977754	2.19 (3.61)
α_D	69.1	175.6	−554.976388	3.04 (4.46)
Chloroform mimicking environment				
β	−95.8	177.2	−554.991072	0.00 (1.65)
C7eq	−111.7	83.3	−554.990929	0.09 (1.74)
α_L	60.0	32.8	−554.988224	1.79 (3.44)
α_D	69.4	176.6	−554.986972	2.57 (4.22)
Water mimicking environment				
β	−95.4	179.8	−554.996983	0.00 (1.22)
$\beta 2$	−118.4	38.1	−554.996738	0.15 (1.37)
α_L	59.4	30.8	−554.993719	2.05 (3.27)
α_D	64.6	−170.4	−554.993530	2.17 (3.39)

and the conformers β and C7eq are deviated. Table 4 shows that the values of the torsion angle ϕ are considerably limited. Only values of about -116° or 55° are adopted, which correspond to the conformers β, $\beta 2$ and α_L, α_D, respectively. The introduction of the bulky methyl group at the *N*-terminal amide results in the absence of the low energy conformers C5 and α_R. It also changes the geometry of the conformers β and C7eq, and as a result their stabilisation decreases. However, it does not change the conformers α_L and α_D much. Thus, the gap in energy between the conformers diminishes and the conformer α_L, as well as, to a smaller extent, the conformer α_D become accessible.

The theoretical calculations supported by the small number of experimental data reveal that the amino acid residues with a *C*-terminal ester bond and methylated on the *N*-terminal amide will have a considerable tendency to adopt the conformers β, $\beta 2$ and α_L.

Cis-Ac-(Me)Ala-OMe

It is known that methylation of the amide bond increases its tendency to adopt the configuration *cis*. The results of the database search indicate that ~20% of the methylated amide bonds preceding the ester bond in the main chain adopt the configuration *cis* (Table 1). Therefore, the conformational properties of *cis*-Ac-(Me)Ala-OMe were also analysed (Figure 6). Four conformers were found (Table 6). *In vacuo* and in the chloroform mimicking environment these are: C7eq, β, α_L and α_D (Figure 6(a)). In the water mimicking environment, the conformer C7eq changes into the conformer $\beta 2$ (Figure 6(b)). The environment seems not to influence the remaining conformers β, α_L and α_D much and the changes in their torsion angles are small. In the polar environment the conformer β becomes the lowest in energy and the order of stability is as follows: β, $\beta 2$/C7eq, α_L and α_D. The number of solid state conformations is very small (32), however the majority of them are placed in the region of the lowest energy conformer β.

Comparisons of Figures 5 and 6 as well as Tables 5 and 6 show that the changes of the configuration *trans*/*cis* of the *N*-terminal amide of the Ac-(Me)Ala-OMe molecule do not considerably

Journal of PeptideScience

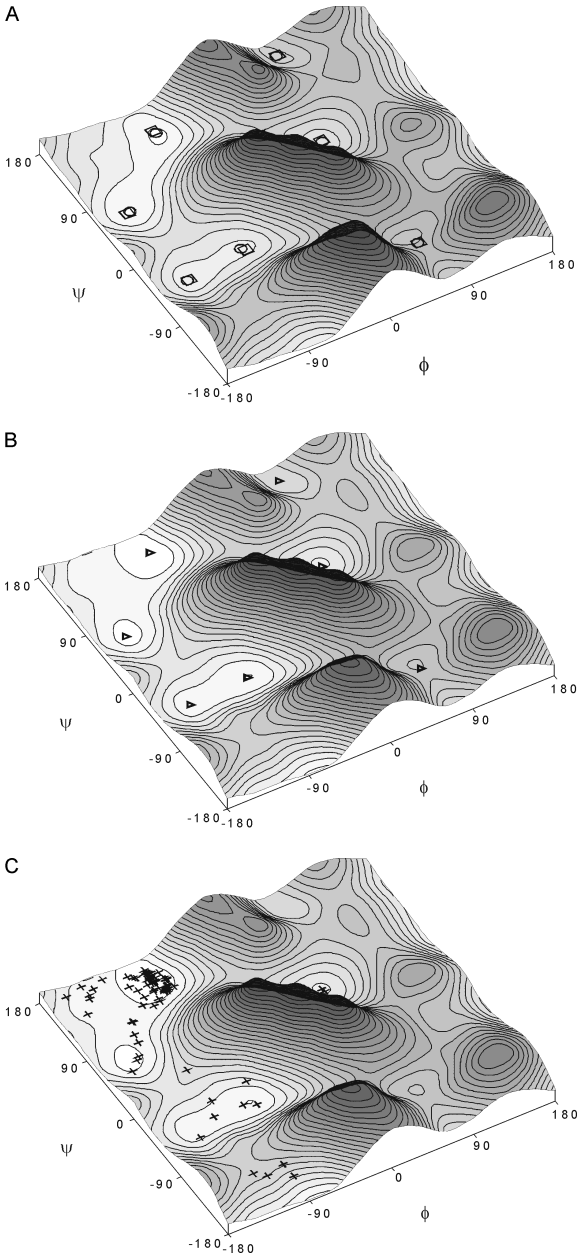

Figure 7. The ϕ, ψ potential energy surfaces of the Ac-[psi](COO)Ala-NMe2 molecule: (a) plot calculated *in vacuo*, conformers calculated *in vacuo* (○) and in a chloroform mimicking environment (□), (b) plot and conformers in a water mimicking environment and (c) distribution of the solid state conformation of the -[psi](COO)Xaa-NR- residue (non-Gly, non-Pro) presented on the plot calculated in a water mimicking environment.

change the shape of the potential energy surfaces and the number of conformers. Particularly, this can be seen in the water mimicking environment. The most occupied areas are the regions of the lowest energy conformers β and $\beta 2$. The tendency to adopt the conformer α_L should be much smaller as the gap in energy between the conformers β, $\beta 2$ and α_L, α_D is greater than in the case when the configuration *trans* of the *N*-terminal amide is adopted.

Comparison of the stabilities of the conformers *trans* and *cis* of the Ac-(Me)Ala-OMe molecule (Table 6, value in parenthesis) shows that the conformer *trans* always has lower energy than

Table 7. Conformers of the CH_3-[psi](COO)Ala-NMe_2 molecule

Conformer	ϕ (°)	ψ (°)	Energy (Hartrees)	ΔE (kcal/mol)
in vacuo				
β	−68.5	149.4	−554.986787	0.00
$\beta 2$	−143.7	69.3	−554.986686	0.06
α'	−145.9	−44.4	−554.984323	1.54
α_R	−80.4	−33.5	−554.983830	1.85
α_L	56.9	47.8	−554.981473	3.33
α_D	72.6	163.5	−554.977986	5.52
α_D	58.8	−131.4	−554.974339	7.81
Chloroform mimicking environment				
β	−70.2	152.7	−554.996766	0.00
$\beta 2$	−147.3	68.3	−554.995601	0.73
α_R	−77.0	−37.2	−554.994234	1.59
α'	−144.0	−44.4	−554.993992	1.74
α_L	56.9	49.5	−554.991334	3.41
α_D	73.9	163.7	−554.988822	4.98
α_D	60.0	−131.5	−554.983627	8.24
Water mimicking environment				
β	−71.6	156.8	−555.002617	0.00
$\beta 2$	−148.5	68.6	−555.001114	0.94
α_R	−76.8	−38.3	−555.000686	1.21
α'	−143.4	−44.2	−554.999666	1.85
α_L	56.5	50.3	−554.997926	2.94
α_D	74.7	164.3	−554.994877	4.85
α_D	60.2	−132.0	−554.989486	8.24

the analogous conformer *cis*. Furthermore, the highest energy conformer, *trans,* is still more favored than the lowest conformer *cis*. Therefore, the presence of the *C*-terminal ester should not increase the tendency of the *N*-terminal methylated amide bond to adopt the configuration *cis*.

Ac-[psi](COO)-Ala-Me_2

Figure 7 and Table 7 present the conformational preferences of the Ac-[psi](COO)-Ala-Me_2 molecule, the model of the residue having an *N*-terminal ester bond, and simultaneously, having the *C*-terminal amide methylated. The calculations reveal seven conformers: β, $\beta 2$, α', α_R, α_L and two conformers α_D. The environment seems not to influence the number of conformers or their geometry. Generally, the energy order is maintained. The most stable are the conformers β and $\beta 2$. The gap in energy between these conformers increases with the increase in the polarity of the environment, and in water the difference in energy reaches the value of about 0.9 kcal/mol. The conformers α' and α_R are in the middle in the energy order. The gap in energy between the lowest conformer β and the conformer α' increases with the increase in the polarity of the environment, whereas the opposite tendency can be observed in the case of the conformer α_R. Thus, in the solvent environment, the conformer α_R is lower in energy than the conformer α'. The remaining conformers α_L and α_D are considerable higher in energy, regardless of the simulated environment.

The number of solid state conformations found in the CSD base is limited. Nevertheless, it confirms the results of the calculations. The majority of the -[psi](COO)-Ala-NMe- residues adopt the

conformation placed in the region of the lowest conformer β (48 of 78 residues found). The conformations which correspond to the conformers $\beta 2$, α', α_R are also present.

Comparison of conformational properties show that the Ac-[psi](COO)-Ala-NMe_2 and the Ac-[psi](COO)-Ala-NHMe molecules reveal some similarities in the pattern of the conformers (Figures 4 and 7, Tables 4 and 7). However, for the Ac-[psi](COO)-Ala-NMe_2 molecule the conformer β is the lowest in energy, regardless of the environment. The conformers α' and α_R have a higher energy than those of the Ac-[psi](COO)-Ala-NHMe molecule. It is also shown by the distribution of the solid state conformations (Figures 4(c) and 7(c)). Within the -[psi](COO)-Ala-NMe- residue any internal N–H···O bond/interaction can be created. As a consequence, the conformers α' and α_R cannot stabilised by five-membered N–H···O interaction, as in the case of the conformers of the analogous -[psi](COO)-Ala-NH- residue.

Conclusion

The introduction of the ester bond in the peptide main chain has a different influence on the residues following and preceding in the sequence. The residues with the *C*-terminal ester bond prefer the conformations β, (ϕ, $\psi = -78^\circ$, 158°), C5 (ϕ, $\psi = -138^\circ$, 165°), and α_R (ϕ, $\psi = -88^\circ$, -18°). Thus, they have properties similar to the standard, non-modified, non-Gly, non-Pro, amino acid residues. The residues with the *N*-terminal ester bond also display a tendency to adopt the conformations β (ϕ, $\psi = -71^\circ$, 149°) and α_R (ϕ, $\psi = -80^\circ$, -29°). However, they prefer the unique conformer α' (ϕ, $\psi = -146^\circ$, -12°) instead of the conformation C5.

Methylation of the neighbouring amide significantly changes the conformational properties of the affected residue. The residues with *N*-terminal methylated amide and *C*-terminal ester linkage prefer the conformations β (ϕ, $\psi = -109^\circ$, 175°), $\beta 2$ (ϕ, $\psi = -118^\circ$, 31°), and interestingly, the conformation α_L (ϕ, $\psi = 52^\circ$, 42°), which is much more easily accessible than the analogous conformation of the standard amino acids. When the methylated amide adopts the configuration *cis*, only the conformations β (ϕ, $\psi = -95^\circ$, 180°) and $\beta 2$ (ϕ, $\psi = -118^\circ$, 38°) are preferred. However, it should be noted that the neighbouring ester linkage does not increase the tendency towards the configuration *cis*. The residues with *C*-terminal methylated amide and *N*-terminal ester linkage prefer primarily the conformation β (ϕ, $\psi = -72^\circ$, 157°).

Naturally occurring depsipeptides reveal a broad spectrum of biological activity. The structural complexity of these compounds, containing many modifications, makes investigations into their structure–activity relationship (SAR) difficult. Description of the selective structural modifications can be helpful in understanding their biological functions. It is suggested that the residues which have an ester bond as well as both ester and methylated amide bonds have different conformational properties. The location of these modifications (*N*-terminus or *C*-terminus) is also important for the conformational properties of the affected residue. This work is a contribution to the knowledge around the structural varieties of natural products, which can be further applied in the design of new bioactive peptides.

Acknowledgement

The author gratefully acknowledges the Academic Computer Centre CYFRONET AGH of Kraków for the grant MNiSW/SGI3700/UOpolski/009/2007.

References

1 Ivanov VT, Mikhaleva II, Methods of organic chemistry (Houben-Weyl) Tom E22c. In: Goodman M, Felix A, Toniolo C (eds). *Synthesis of Peptides and Peptidomimetics*. Georg Thieme Verlag: Stuttgart; 2003; p 272.
2 URL: http://www.chem.qmul.ac.uk/iupac/AminoAcid (3AA-19.6. Depsipeptides).
3 Ballard CE, Yu H, Wang B. Recent developments in depsipeptide research. *Curr. Med. Chem.* 2002; **9**: 471–498.
4 Sarabia F, Chammaa S, Ruiz AS, Ortiz LM, Herrera FJL. Chemistry and biology of cyclic depsipeptides of medicinal and biological interest. *Curr. Med. Chem.* 2004; **11**: 1309–1332.
5 Nakajima H, Kim YB, Terano H, Yoshida M, Horinouchi S. FR901228, a potent antitumor antibiotic, is a novel histone deacetylase inhibitor. *Exp. Cell Res.* 1998; **241**: 126–133.
6 Hale KJ, Manaviazar S, George JH, Walters MA, Dalby SM. Total synthesis of (+)-azinothricin and (+)-kettapeptin. *Org. Lett.* 2009; **11**: 733–736.
7 Bishara A, Rudi A, Aknin M, Neumann D, Ben-Califa N, Kashman Y. Taumycins A and B, two bioactive lipodepsipeptides from the madagascar sponge *Fascaplysinopsis sp*. *Org. Lett.* 2008; **10**: 4307–4309.
8 Ohlendorf B, Kehraus S, König GM. Myxochromide B_3, a new member of the myxochromide family of secondary metabolites. *J. Nat. Prod.* 2008; **71**: 1708–1713.
9 Oh D-C, Jensen PR, Fenical W. Zygosporamide, a cytotoxic cyclic depsipeptide from the marine-derived fungus *Zygosporium masonii*. *Tetrahedron Lett.* 2006; **47**: 8625–8628.
10 Belofsky GN, Jensen PR, Fenical W. Sansalvamide: a new cytotoxic cyclic depsipeptide produced by a marine fungus of the genus *Fusarium*. *Tetrahedron Lett.* 1999; **40**: 2913–2916.
11 Kuisle O, Quio E, Riguera R. A general methodology for automated solid-phase synthesis of depsides and depsipeptides. Preparation of a valinomycin analogue. *J. Org. Chem.* 1999; **64**: 8063–8075.
12 Suwan S, Isobe M, Ohtani I, Agata N, Mori M, Ohta M. Structure of cereulide, a cyclic dodecadepsipeptide toxin from *Bacillus cereus* and studies on NMR characteristics of its alkali metal complexes including a conformational structure of the K+ complex. *J. Chem. Soc. Perkin Trans.* 1995; **1**: 765–775.
13 Pettit GR, Tan R, Melody N, Kielty JM, Pettit RK, Herald DL, Tucker BE, Mallavia LP, Doubek DL, Schmidt JM. Antineoplastic agents. Part 409: isolation and structure of montanastatin from a terrestrial *actinomycete*. *Bioorg. Med. Chem.* 1999; **7**: 895–899.
14 Cavelier F, Verducci J, André F, Haraux F, Sigalat C, Traris M, Vey A. Natural cyclopeptides as leads for novel pesticides: tentoxin and destruxin. *Pestic. Sci.* 1998; **52**: 81–89.
15 Feng Y, Carroll AR, Pass DM, Archbold JK, Avery VM, Quinn RJ. Polydiscamides B-D from a marine sponge *Ircinia sp.* as Potent human sensory neuron-specific G protein coupled receptor agonists. *J. Nat. Prod.* 2008; **71**: 8–11.
16 Nogle LM, Williamson RT, Gerwick WH. Somamides A and B, two new depsipeptide analogues of dolastatin 13 from a Fijian cyanobacterial assemblage of *Lyngbya majuscula* and *Schizothrix* species. *J. Nat. Prod.* 2001; **64**: 716–719.
17 Kisugi T, Okino T. Micropeptins from the Freshwater cyanobacterium *Microcystis aeruginosa* (NIES-100). *J. Nat. Prod.* 2009; **72**: 777–781.
18 Itou Y, Ishida K, Shin HJ, Murakami M. Oscillapeptins A to F, serine protease inhibitors from the three strains of *Oscillatoria agardhii*. *Tetrahedron* 1999; **55**: 6871–6882.
19 Rangel M, Prado MP, Konno K, Naoki H, Freitas JC, Machado-Santelli GM. Cytoskeleton alterations induced by Geodia corticostylifera depsipeptides in breast cancer cells. *Peptides* 2006; **27**: 2047–2057.
20 Nakadate S, Nozawa K, Sato H, Horie H, Fujii Y, Nagai M, Hosoe T, Kawai K-i, Yaguchi T. Antifungal cyclic depsipeptide, eujavanicin a, isolated from *Eupenicillium Javanicum*. *J. Nat. Prod.* 2008; **71**: 1640–1642.
21 Roy MC, Ohtani II, Ichiba T, Tanaka J, Satari R, Higa T. New cyclic peptides from the indonesian sponge *Theonella swinhoei*. *Tetrahedron* 2000; **56**: 9079–9092.
22 Zampella A, Randazzo A, Borbone N, Luciani S, Trevisi L, Debitus C, D'Auria MV. Isolation of callipeltins A-C and of two new open-chain derivatives of callipeltin A from the marine sponge *Latrunculia sp.* A revision of the stereostructure of callipeltins. *Tetrahedron Lett.* 2002; **43**: 6163–6166.

23 Ghosh AK, Xu C-X. A convergent synthesis of the proposed structure of antitumor depsipeptide stereocalpin A. *Org. Lett.* 2009; **11**: 1963–1966.
24 Plaza A, Bifulco G, Keffer JL, Lloyd JR, Baker HL, Bewley CA. Celebesides A-C and theopapuamides B-D, depsipeptides from an Indonesian sponge that inhibit HIV-1 entry. *J. Org. Chem.* 2009; **74**: 504–512.
25 Sitachitta N, Williamson RT, Gerwick WH. Yanucamides A and B, two new depsipeptides from an assemblage of the marine cyanobacteria *Lyngbya majuscula* and *Schizothrix* species. *J. Nat. Prod.* 2000; **63**: 197–200.
26 Boger DL, Ledeboer MW, Kume M, Searcey M, Jin Q. Total synthesis and comparative evaluation of luzopeptin A-C and quinoxapeptin A-C. *J. Am. Chem. Soc.* 1999; **121**: 11375–11383.
27 Tripathi A, Puddick J, Prinsep MR, Lee PPF, Lik TT. Hantupeptin A, a cytotoxic cyclic cepsipeptide from a singapore collection of *Lyngbya majuscule*. *J. Nat. Prod.* 2009; **72**: 29–32.
28 Vervoort H, Fenical W, Epifanio RDA. Tamandarins A and B: new cytotoxic depsipeptides from a Brazilian ascidian of the family didemnidae. *J. Org. Chem.* 2000; **65**: 782–792.
29 Ferrié L, Reymond S, Capdevielle P, Cossy J. Total synthesis of (−) -spongidepsin. *Org. Lett.* 2006; **8**: 3441–3443.
30 Dang J, Aurelio L, Hughes AB, Brownlee RTC. Solution structures by NMR of a novel antifungal drug: petriellin A. *Org. Biomol. Chem.* 2006; **4**: 3802–3807.
31 Horgen FD, Yoshida WY, Scheuer PJ, Malevamides A-C, New depsipeptides from the marine cyanobacterium *Symploca laete-viridis*. *J. Nat. Prod.* 2000; **63**: 461–467.
32 Gunasekera SP, Ritson-Williams R, Paul VJ. Carriebowmide, a new cyclodepsipeptide from the marine cyanobacterium *Lyngbya polychroa*. *J. Nat. Prod.* 2008; **71**: 2060–2063.
33 Lee H-S, Song H-H, Jeong J-H, Shin C-G, Choi S-U, Lee C. Cytotoxicities of enniatins H, I, and MK1688 from *Fusarium oxysporum* KFCC 11363P. *Toxicon* 2008; **51**: 1178–1185.
34 Müller J, Feifel SC, Schmiederer T, Zocher R, Süssmuth RD. In vitro synthesis of new cyclodepsipeptides of the PF1022-type: probing the α-D-hydroxy acid tolerance of PF1022 synthetase. *ChemBioChem* 2009; **10**: 323–328.
35 Sasaki T, Takagi M, Yaguchi T, Miyadoh S, Okada T, Koyama M. A new anthelmintic cyclodepsipeptide, PF1022A. *J. Antibiot.* 1992; **45**: 692–697.
36 Monma S, Sunazuka T, Nagai K, Arai T, Shiomi K, Matsui R, Ohmura S. Verticilide: elucidation of absolute configuration and total synthesis. *Org. Lett.* 2006; **8**: 5601–5604.
37 In Y, Ishida T, Takesako K. Unique molecular conformation of aureobasidin A, a highly amide N-methylated cyclic depsipeptide with potent antifungal activity: X-ray crystal structure and molecular modeling studies. *J. Peptide Res.* 1999; **53**: 492–500.
38 Sone H, Nemoto T, Ishiwata H, Ojika M, Yamada K. Isolation, structure, and synthesis of dolastatin D, a cytotoxic cyclic depsipeptide from the sea hare *Dolabella auricularia*. *Tetrahedron Lett.* 1993; **34**: 8449–8452.
39 Pettit GR, Xu J-P, Hogan F, Cerny RL. Isolation and structure of dolastatin 17. *Heterocycles* 1998; **47**: 491–496.
40 Han B, Goeger D, Maier CS, Gerwick WH. The wewakpeptins, cyclic depsipeptides from a Papua New Guinea collection of the marine cyanobacterium *Lyngbya semiplena*. *J. Org. Chem.* 2005; **70**: 3133–3139.
41 Ingwall RT, Goodman M. Polydepsipeptides. III. Theoretical conformational analysis of randomly coiling and ordered depsipetide chains. *Macromolecules* 1974; **7**: 598–605.
42 Ingwall RT, Gilon C, Goodman M. Polydepsipeptides. 5. Experimental conformational analysis of poly(l-alanyl-l-lactic acid) and related model compounds. *Macromolecules* 1976; **9**: 802–808.
43 Zhang J, King M, Suggs L, Ren P. Molecular modeling of conformational properties of oligodepsipeptides. *Biomacromolecules* 2007; **8**: 3015–3024.
44 Kang YK, Byun BJ. Conformational preferences and cis-trans isomerization of L-lactic acid residue. *J. Phys. Chem. B* 2008; **112**: 9126–9134.
45 URL: www.ccdc.cam.ac.uk The Cambridge Structural Database CSD version 5.30 (November 2008).
46 URL: http://www.chem.qmul.ac.uk/iupac/AminoAcid (3AA-19.7. Peptide Analogues).
47 Frisch MJ, Trucks GW, Schlegel HB, Scuseria GE, Robb MA, Cheseman JR, Montgomery Jr JA, Vreven T, Kudin KN, Burant JC, Millam JM, Iyengar SS, Tomasi J, Barone V, Mennucci B, Cossi M, Scalmani G, Rega N, Petersson GA, Nakatsuji H, Hada M, Ehara M, Toyota K, Fukuda R, Hasegawa J, Ishida M, Nakajima T, Honda Y, Kitao O, Nakai H, Klene M, Li X, Knox JE, Hratchnian HP, Cross JB, Adamo C, Jaramillo J, Gomperts R, Stratmann RE, Yazyev O, Austin AJ, Cammi R, Pomelli C, Ochterski JW, Ayala PY, Morokuma K, Voth GA, Salvador P, Dannenberg JJ, Zakrzewski VG, Dapprich S, Danields AD, Strain MC, Farkas O, Malick DK, Rabuck AD, Raghavachari K, Foresman JB, Ortiz JV, Cui Q, Baboul AG, Clifford S, Cioslowski J, Stefanov J, Liu G, Liashenko A, Piskorz P, Komaromi I, Martin RL, Fox DJ, Keith T, Al-Laham MA, Peng CY, Nanayakkara A, Challacombe M, Gill PMW, Johnson B, Chen W, Wong MW, Gonzalex C, Pople JA. *Gaussian'03 Revision C.02*, Gaussian Inc.: Pittsburgh, PA; 2003.
48 Miertus S, Tomasi J. Approximateevaluationsof theelectrostatic free energy and internal energy changes in solution processes. *Chem. Phys.* 1982; **65**: 239–245.
49 Tomasi J, Mennucci B, Cammi R. Quantum mechanical continuum salvation models. *Chem. Rev.* 2005; **105**: 2999–3093.
50 Vargas R, Garza J, Hay BP, Dixon DA. Conformational study of the alanine dipeptide at the MP2 and DFT levels. *J. Phys. Chem. A* 2002; **106**: 3213–3218.
51 Lovell SC, Davis IW, Arendall III WB, de Bakker PIW, Word JM, Prisant MG, Richardson JS, Richardson DC. Structure Validation by Cα Geometry: ϕ,ψ and Cβ Deviation. *PROTEINS: Structure, Function, and Genetics* 2003; **50**: 437–450.

